Yifan Zhou
State Key Lab for Strength and Vibration of Mechanical Structures,
International Center for Applied Mechanics,
Department of Engineering Mechanics,
Xi'an Jiaotong University,
Xi'an 710049, China
e-mail: 773922409@qq.com

Wenlei Zhang
State Key Lab for Strength and Vibration of Mechanical Structures,
International Center for Applied Mechanics,
Department of Engineering Mechanics,
Xi'an Jiaotong University,
Xi'an 710049, China
e-mail: zhangwenlei@stu.xjtu.edu.cn

Jian Hu
State Key Lab for Strength and Vibration of Mechanical Structures,
International Center for Applied Mechanics,
Department of Engineering Mechanics,
Xi'an Jiaotong University,
Xi'an 710049, China
e-mail: hujian@mail.xjtu.edu.cn

Jingda Tang
State Key Lab for Strength and Vibration of Mechanical Structures,
International Center for Applied Mechanics,
Department of Engineering Mechanics,
Xi'an Jiaotong University,
Xi'an 710049, China
e-mail: tangjd@mail.xjtu.edu.cn

Chenyu Jin
State Key Lab for Strength and Vibration of Mechanical Structures,
International Center for Applied Mechanics,
Department of Engineering Mechanics,
Xi'an Jiaotong University,
Xi'an 710049, China
e-mail: jinchenyu7@stu.xjtu.edu.cn

Zhigang Suo[1]
John A. Paulson School of Engineering and Applied Sciences,
Kavli Institute for Bionano Science and Technology,
Harvard University,
MA 02138
e-mail: suo@seas.harvard.edu

Tongqing Lu[1]
State Key Lab for Strength and Vibration of Mechanical Structures,
International Center for Applied Mechanics,
Department of Engineering Mechanics,
Xi'an Jiaotong University,
Xi'an 710049, China
e-mail: tongqinglu@mail.xjtu.edu.cn

The Stiffness-Threshold Conflict in Polymer Networks and a Resolution

Stiffness and fatigue threshold are important material parameters in load-carrying applications. However, it is impossible to achieve both high stiffness and high threshold for single-network elastomers and single-network hydrogels. As the polymer chain length increases, the stiffness reduces, but the threshold increases. Here, we show that this stiffness-threshold conflict is resolved in double-network hydrogels, where the stiffness depends on the short-chain network, but the threshold depends on the long-chain network. Experimental data in the literature have shown that the stiffness of the hydrogels is inversely proportional to chain length of the short-chain network. In this paper we measure the threshold of PAAm-PAMPS hydrogels with five different chain lengths of the long-chain network. We find that the threshold is proportional to 1/2 power of the chain length of the long-chain network. The resolution of the conflict enables the design of elastomers and hydrogels to achieve both high stiffness and high threshold. [DOI: 10.1115/1.4044897]

Keywords: hydrogel, fatigue, stiffness, double network

[1]Corresponding authors.

Contributed by the Applied Mechanics Division of ASME for publication in the JOURNAL OF APPLIED MECHANICS. Manuscript received July 13, 2019; final manuscript received August 23, 2019; published online September 18, 2019. Assoc. Editor: Yong-Wei Zhang.

1 Introduction

A load-carrying material is commonly required to sustain cyclic loads without damage. Two material properties are of particular importance: stiffness to resist excessive deformation and fatigue threshold to resist crack growth. Both high stiffness and high threshold are desired, but a stiffness-threshold conflict exists for single-network elastomers and single-network hydrogels. A single-network material cannot achieve both high stiffness and high threshold. The conflict results from a fundamental fact: both stiffness E and threshold Γ_0 of a single-network material are controlled by the chain length n of the same network, $E \sim 1/n$ and $\Gamma_0 \sim \sqrt{n}$ [1,2].

We hypothesize that the stiffness-threshold conflict is resolved in double-network materials. In a material of two interpenetrating networks, one network has short chains of length n_A and the other network has long chains of n_B. We expect that the stiffness is controlled by the short-chain network, $E \sim 1/n_A$, and the threshold is controlled by the long-chain network, $\Gamma_0 \sim \sqrt{n_B}$. Once the stiffness and threshold are controlled by different networks, the stiffness-threshold conflict no longer exists.

We test this hypothesis by using the double-network hydrogels discovered by Gong et al. [3]. Experimental data in the literature have shown the stiffness of these hydrogels is inversely proportional to the chain length of the short-chain network [4]. In this paper we measure the threshold of the hydrogels with five different chain lengths of the long-chain network. We find that the threshold is proportional to 1/2 power of the chain length of the long-chain network. The resolution of the conflict enables the design of elastomers and hydrogels to achieve both high stiffness and high threshold.

2 The Stiffness-Threshold Conflict in Polymer Networks

The stiffness-threshold conflict is inherent to single-network materials. An elastomer is a crosslinked network of flexible polymer chains. Young's modulus is estimated by $E = 3kT/(Vnl)$, where kT is the temperature in the unit of energy, V the volume per monomer, n the number of monomers per polymer chain, and l the length of the monomer unit [1]. The fatigue threshold is estimated by the Lake-Thomas model, $\Gamma_0 = \alpha\sqrt{n}lJ/V$, where J is the energy per covalent bond and α a dimensionless number of order unity [2]. As the chain length n increases, the stiffness decreases, $E \sim 1/n$, but the threshold increases, $\Gamma_0 \sim \sqrt{n}$, so that $\Gamma_0 \sim E^{-1/2}$. Consequently, single-network elastomers can never achieve high stiffness and high threshold simultaneously. This stiffness-threshold conflict has been experimentally confirmed for elastomers (Fig. 1) [5].

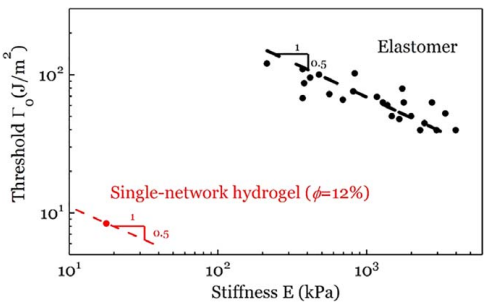

Fig. 1 Stiffness-threshold conflict in polymer networks. For single-network elastomers, the experimental data fall onto a straight line with a slope of −1/2. Included are data of seven kinds of elastomers [5]. Stiffness-threshold data for single-network hydrogels have not been studied. Here, a single red dot represents experimental data reported in Ref. [6] and a dashed line of a slope −1/2 is plotted through the data point.

The stiffness-threshold conflict also exists for single-network hydrogels. A single-network hydrogel is an aggregate of water molecules and one flexible polymer network. Young's modulus is estimated by $E = 3\phi^{1/3}kT/(Vnl)$, and the threshold is estimated by $\Gamma_0 = \alpha\phi\sqrt{n}lJ/V$, where ϕ is the volume fraction of the polymer [7–9]. At a given volume fraction of the polymer, the stiffness-threshold conflict in hydrogels is the same as that in elastomers, that is, $\Gamma_0 \sim E^{-1/2}$. The experimental data of stiffness and threshold for single-network hydrogels have not been systematically reported. One red dot marked in Fig. 1 corresponds to a stiffness of 18 kPa and a threshold of 8.4 J/m^2 for a polyacrylamide (PAAm) hydrogel with a volume fraction of polymer of 12% [6]. Through this point, we plot a red dashed line with a slope of −1/2, which shifts from the black dashed line for the elastomers by roughly an order of magnitude. It is understandable that no one has ever tried to improve the fatigue threshold of single-network PAAm hydrogel by simply increasing the chain length, because the PAAm hydrogel with a very long chain has negligible stiffness. On the other hand, the PAAm hydrogels with shorter chains and higher stiffness are very brittle.

3 A Resolution of the Stiffness-Threshold Conflict

The stiffness-threshold conflict results from a fundamental fact: both material properties of a single-network material are controlled by the chain length of the same network, $E \sim 1/n$ and $\Gamma_0 \sim \sqrt{n}$. We hypothesize that this conflict is resolved in double-network materials. Double-network hydrogels have received substantial attention in recent years as they exhibit high toughness [3,10–12]. These tough hydrogels have stimulated many new applications in bioengineering [13,14], soft robotics [15,16], and ionotronic devices [17–20].

We test the hypothesis using the PAAm-PAMPS double-network hydrogels. Such a hydrogel consists of a long-chain, flexible PAAm network and a short-chain, stiff PAMPS network. The two networks interpenetrate in topological entanglement (Fig. 2(*a*)). The short-chain network swells nearly to the breaking point. When the hydrogel is stretched, the PAMPS network sustains most of the load and provides the stiffness. With a larger stretch, the short-chain PAMPS network starts to break while the long-chain network remains nearly intact.

The toughness of a material is measured by the energy needed to extend a crack by a unit area under monotonic loading. The long-chain network transmits the intense stress at the crack front into a large volume of the hydrogel and breaks many short chains. Consequently, the extension of the crack under the monotonic load

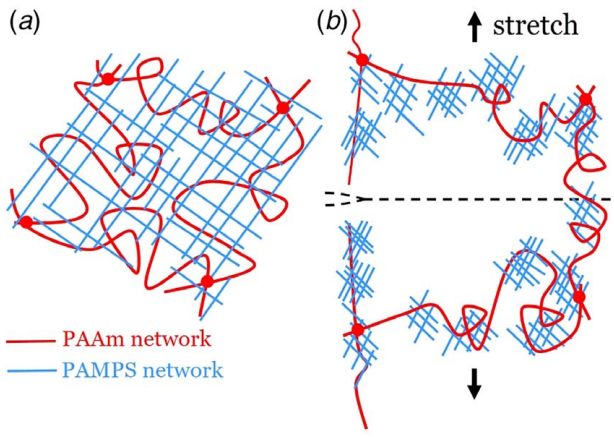

Fig. 2 Schematics of the PAAm-PAMPS double-network hydrogel. (*a*) In the as-prepared state, the PAMPS network and the PAAm network interpenetrate in topological entanglement. (*b*) After prolonged cyclic loads, the PAMPS network breaks into small clusters. A crack advances by breaking a PAAm chain.

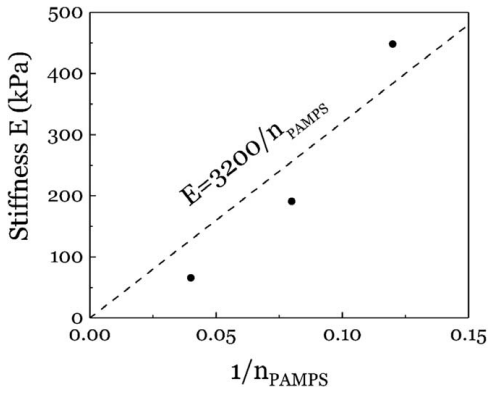

Fig. 3 The stiffness of the PAAm-PAMPS hydrogel as a function of the inverse of the chain length of the PAMPS network

is resisted by the synergy of both short-chain and long-chain networks [21].

The fatigue threshold of a material is measured by subjecting a notched sample under a cyclic load. The threshold is defined by the amplitude of the energy release rate, below which the crack will not extend. Under a cyclic load above the threshold, much of the short-chain network around the crack front breaks into small clusters in previous cycles (Fig. 2(*b*)). Consequently, the threshold of the double network is governed by the long-chain network [22].

To test our hypothesis for the PAAm-PAMPS double-network hydrogels, we need to show that the stiffness is determined by the chain length of the stiff PAMPS network, $E \sim 1/n_{PAMPS}$, and that the threshold is determined by the chain length of the flexible PAAm network, $\Gamma_0 \sim (n_{PAMS})^{1/2}$. The stiffness of the PAAm-PAMPS double-network hydrogel as a function of the chain length of the PAMPS network has been studied by Gong's Group [4]. When the chain length of the PAMPS network was varied, the chain length of the PAAm network and the polymer volume fraction were fixed. The stiffness of the double-network hydrogel is roughly proportional to the inverse of the chain length of the PAMPS network, as we hypothesize (Fig. 3). In this paper, we systematically study the dependence of the threshold of the PAAm-PAMPS double-network hydrogel on the chain length of the PAAm network.

4 Chain Length Dependence on the Threshold of the PAAm-PAMPS Double-Network Hydrogel

Several experimental observations have revealed that the fatigue threshold of a double-network hydrogel is mainly determined by the long-chain polymer network. The introduction of the second network with sacrificial bonds greatly increases the toughness but contributes little to the fatigue threshold. For example, in one experiment, the PAAm hydrogel and the PAAm-PVA hydrogel were used to compare. The PAAm hydrogel has a toughness of 71 J/m^2 and a threshold of 9.5 J/m^2. The PAAm-PVA hydrogel has a toughness of 448 J/m^2 and a threshold of 8.4 J/m^2 [23]. In another experiment, the Na-alginate/PAAm hydrogel and the Ca-alginate/PAAm hydrogel were used to compare. The Na-alginate/PAAm hydrogel has a toughness of 169 J/m^2 and a threshold of 17 J/m^2. The Ca-alginate/PAAm hydrogel has a toughness of 3375 J/m^2 and a threshold of 35 J/m^2 [24]. In the first paper to study the fatigue of PAAm-PAMPS hydrogel, a threshold of 418 J/m^2 was reported [22]. This high value of the threshold is attributed to the very long chain with about 10^5 monomer units.

Figure 2(*b*) shows a crack in a PAAm-PAMPS double-network hydrogel during prolonged cyclic loads. Near the crack front, the stress is concentrated so that all the short-chain PAMPS networks have broken into small clusters and all the remaining is the elastic PAAm network. When the crack further advances, it only activates the inelastic process of scission of the PAAm chain. As analyzed above, when the water content of the hydrogel is fixed, the fatigue threshold is expected to be linear with the square root of the number of monomers of the PAAm chain:

$$\Gamma_0 = C n_{PAAm}^{1/2} \tag{1}$$

where $C = \phi_0^{1/3}\phi^{2/3}\alpha l J/V$ is a constant to be experimentally determined. Here, we also account for the volume fraction of PAAm in the as-prepared hydrogel, ϕ_0, and the volume fraction of PAAm in the swollen hydrogel, ϕ [9].

4.1 Synthesis of the PAAm-PAMPS Double-Network Hydrogel. We synthesized the PAAm-PAMPS double-network hydrogel following a two-step sequential network formation technique developed by Gong et al. [3]. We purchased from Aladdin the following substances: 1-acrylanmido-2-methylpropanesulfonic acid (AMPS, monomer), acrylamide (AAm, monomer), *N*,*N*′-methylenebis (acrylamide) (MBAA, crosslinker), and 2-oxoglutaric acid (OA, initiator). In the first step, we formulated an aqueous solution of 1 M AMPS containing 4 mol% MBAA and 0.1 mol% OA relative to AMPS monomers. In an argon gas environment, we injected the AMPS monomer solution into a plastic mold covered with a pair of 15 mm × 15 mm glass plates and placed the mold under the 15 W and 365 nm ultraviolet lamp for 8 h. A relatively stiff and brittle short-chain network of PAMPS hydrogel was formed. In the second step, we immersed the prepared PAMPS hydrogel in an aqueous solution of 4 M AAm, MBAA, and 0.1 mol% OA for one day. We controlled the chain length of the PAAM network by changing the concentration of the crosslinker, $c_{MBAA} = n_{MBAA}/n_{AAm}$. We used five solutions with c_{MBAA} to be 0.001%, 0.0018%, 0.0036%, 0.01%, and 0.1%. The chain length of the PAAm network is approximately equal to $n_{PAAm} = 1/(2c_{MBAA})$. After the immersion, the gel was sandwiched between two glass plates and placed in the same reaction cell as that in the first step. Subsequently, the prepared gel was immersed in deionized water for one day to swell and to remove the residual reactants. Finally, we obtained the PAAm-PAMPS double-network hydrogels with five different chain lengths of the PAAm network, $n_{PAAm} =$ 500, 5000, 13,889, 27,778, 50,000.

We determined the volume fraction of the PAAm network and PAMPS network by the following method. We prepared two pieces of PAMPS hydrogels with the same chemical components. One piece was dehydrated at 60 °C for half a day to obtain the mass of m_{PAMPS}. We then synthesized a PAAm-PAMPS double-network hydrogel with the other piece. We measured the mass and volume of the double-network hydrogel m_{gel} and V_{gel}. The double-network hydrogel was dehydrated at 60 °C for half a day to obtain the mass of m_{DN}. The volume fraction can be calculated as $\phi_{PAMPS} = m_{PAMPS}/\rho_{PAMPS}V_{gel}$ for the PAMPS network and $\phi_{PAAm} = (m_{DN} - m_{PAMPS})/\rho_{PAAm}V_{gel}$ for the PAAm network in the fully swollen double-network hydrogel. For example, for 0.1% c_{MBAA}, ϕ_{PAMPS} is 1.14% and ϕ_{PAAm} is 9.7%. For 0.001% c_{MBAA}, ϕ_{PAMPS} is 0.9% and ϕ_{PAAm} is 11.8%.

4.2 Fracture Toughness. We use the pure shear test to measure the fracture toughness of the prepared double-network hydrogels [25]. This method requires two sets of samples with identical size and mechanical properties. One set of samples are precut with a crack, the other set of samples are without a crack (Figs. 4(*a*) and 4(*b*)). The uncut samples were prepared as a rectangle sheet (10 mm × 50 mm). The thickness of the hydrogels with $c_{MBAA} =$ 0.1% is 1.43 mm. The thickness of the hydrogels with the other four chain lengths is 1.52 ± 0.02 mm. The cut samples were prepared with the same geometry but with a middle crack of 20 mm cut by a razor blade. Both the cut and uncut samples were fixed to rigid grippers of the tensile tester with a 500 N load cell. The rate of the applied monotonic stretch was set as 30 mm/min. The initial height of each sample is denoted as H, and the height in

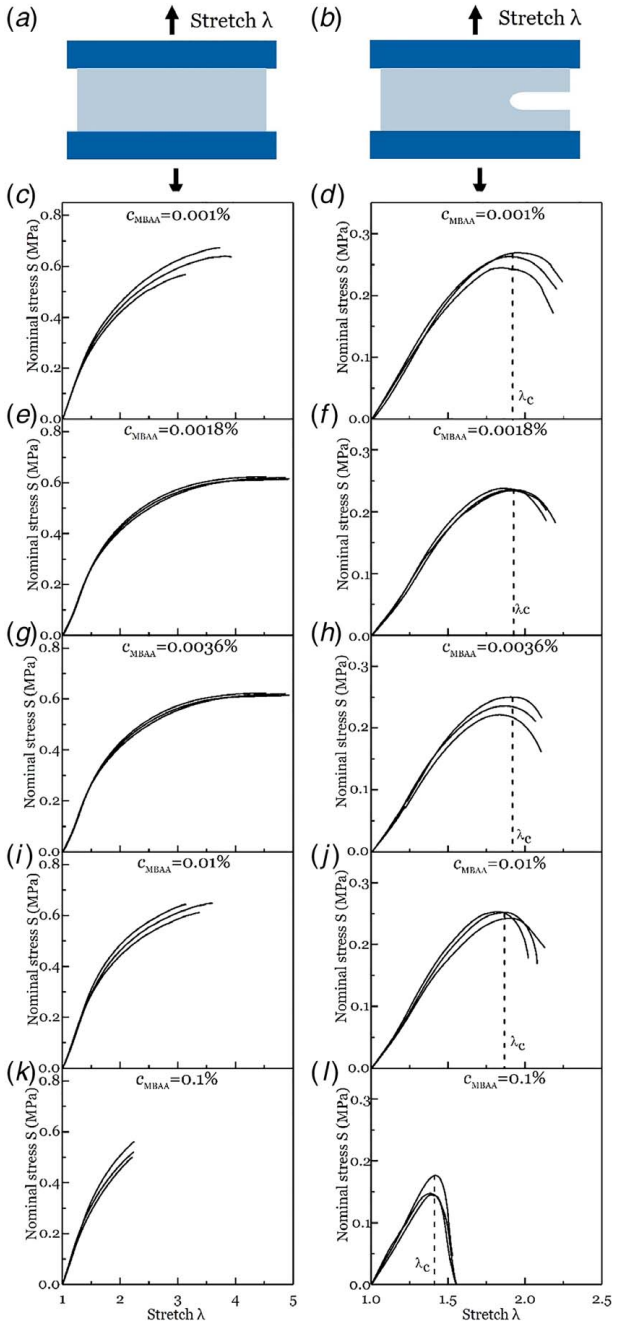

Fig. 4 (*a*) The uncut samples and (*b*) the cut samples of the PAAm-PAMPS hydrogel are subject to a monotonic stretch. (*c*)(*e*)(*g*)(*i*)(*k*) The stress–stretch curves of the uncut samples. (*d*)(*f*)(*h*)(*j*)(*l*) The stress–stretch curves of the cut samples.

the deformed state changes to λH, where λ is the vertical stretch applied to the sample. The horizontal displacement is fixed. The stress–stretch curves of the uncut and cut samples with five different chain lengths are plotted in Fig. 4. For the cut samples, as the applied stretch increased, the crack gradually opened up and then started to advance at a critical stretch λ_c.

The energy release rate G for the pure shear configuration is

$$G = HW(\lambda) \tag{2}$$

where $W(\lambda)$ is the free energy density of the uncut samples, calculated from the integrated area below the stress–stretch curve. The fracture toughness λ is

$$\Gamma = HW(\lambda_c) \tag{3}$$

For the hydrogels with each chain length, three groups of experiments were repeated to obtain the average value. When the chain length of the PAAm network is very low $n_{PAAM} = 500$, the measured toughness is 390 J/m^2. When the chain length increases to 5000, the measured toughness reaches 2550 J/m^2. The increase of toughness from 390 J/m^2 to 2550 J/m^2 due to the increase of the PAAm chain length has been studied before [21]. However, when the chain length further increases, the measured toughness almost does not change, 2599 J/m^2, 2691 J/m^2, and 2841 J/m^2. This is because the high toughness comes from the energy dissipation of the PAMPS network, and the further increase of PAAm chain will not influence the dissipation process.

4.3 Fatigue Damage of Uncut Samples. We next apply triangular cyclic loads to the uncut samples of the double-network hydrogel. The setup is the same as shown in Fig. 4. Following the previous study on the fatigue of hydrogels [6,7,22,23], we set the applied minimum stretch $\lambda_{\min}$ as 1 and vary the maximum stretch $\lambda_{\max}$. The hydrogel with $c_{MBAA} = 0.1\%$ is brittle and its rupture stretch is about 2.2 (Fig. 4(*k*)). The loading rate for the samples of $c_{MBAA} = 0.1\%$ was set as 1 mm/s. The loading rate for the other four kinds of hydrogel samples was set as 3 mm/s. To reduce dehydration during the test, we placed the sample in a sealed acrylic chamber and sprayed droplets of water onto it. We measured the mass of samples before and after the fatigue test. The difference is less than 5%.

Figures 5(*a*)(*c*)(*e*)(*g*)(*i*) show the stress–stretch curves under cyclic loads for the five kinds of samples. The hydrogels with $c_{MBAA} = 0.1\%$ show a very small hysteresis. The other hydrogels show a significant hysteresis in the first cycle and almost reach a steady state after 2000 cycles. The large hysteresis is due to the partial fracture of the PAMPS network. When the hysteresis is small, the material behaves elastically and the energy release rate represents the comprehensive load to advance the crack. We use the data at the 2000th cycle to calculate the energy release rate. In each experiment, the residual stretch was observed. Figures 5–10 show the stress–stretch curves for each kind of samples with different applied $\lambda_{\max}$.

4.4 Fatigue Fracture of Cut Samples. The same cyclic loading profile as above was applied to the cut samples. A video camera (Nikon 5200) was used to record the extension of crack. The extension of crack as a function of the number of cycles is given in Fig. 11. When the applied maximum stretch was close to the critical stretch of the cut sample, the crack grew rapidly in the first cycle. After that the crack extension rate was much lower and gradually reached a steady state. When the applied maximum stretch was below the critical stretch of the cut sample, the difference of extension rate between the first cycle and the subsequent cycles was small. In most cases, after 2000 cycles of loading, the crack extension rate was approximately linearly related to the number of cycles. The total number of cycles of different samples range from 4000 to 10,000. The resolution of the imaging process to detect crack growth is 10^{-4} m. As a result, the minimum length of crack extension per cycle that we can observe is on the order of 10^{-7} m. When the applied energy release rate is higher, the crack extends faster. The extension of crack per cycle of the five kinds of hydrogel samples is plotted as a function of the applied energy release rate in Figs. 5(*b*)(*d*)(*f*)(*h*)(*j*). This *G-dc/dN* plot was first used by Thomas in 1958 to describe the fatigue fracture of elastomers [26].

5 Results and Discussions

We linearly extrapolate the data points on the *G-dc/dN* plane and take the intercept on the *G* axis as the threshold of fatigue fracture Γ_0. The threshold is 266.2 J/m^2 for the double-network hydrogel with $c_{MBAA} = 0.001\%$, 223.8 J/m^2 for $c_{MBAA} = 0.0018\%$, 155.4 J/

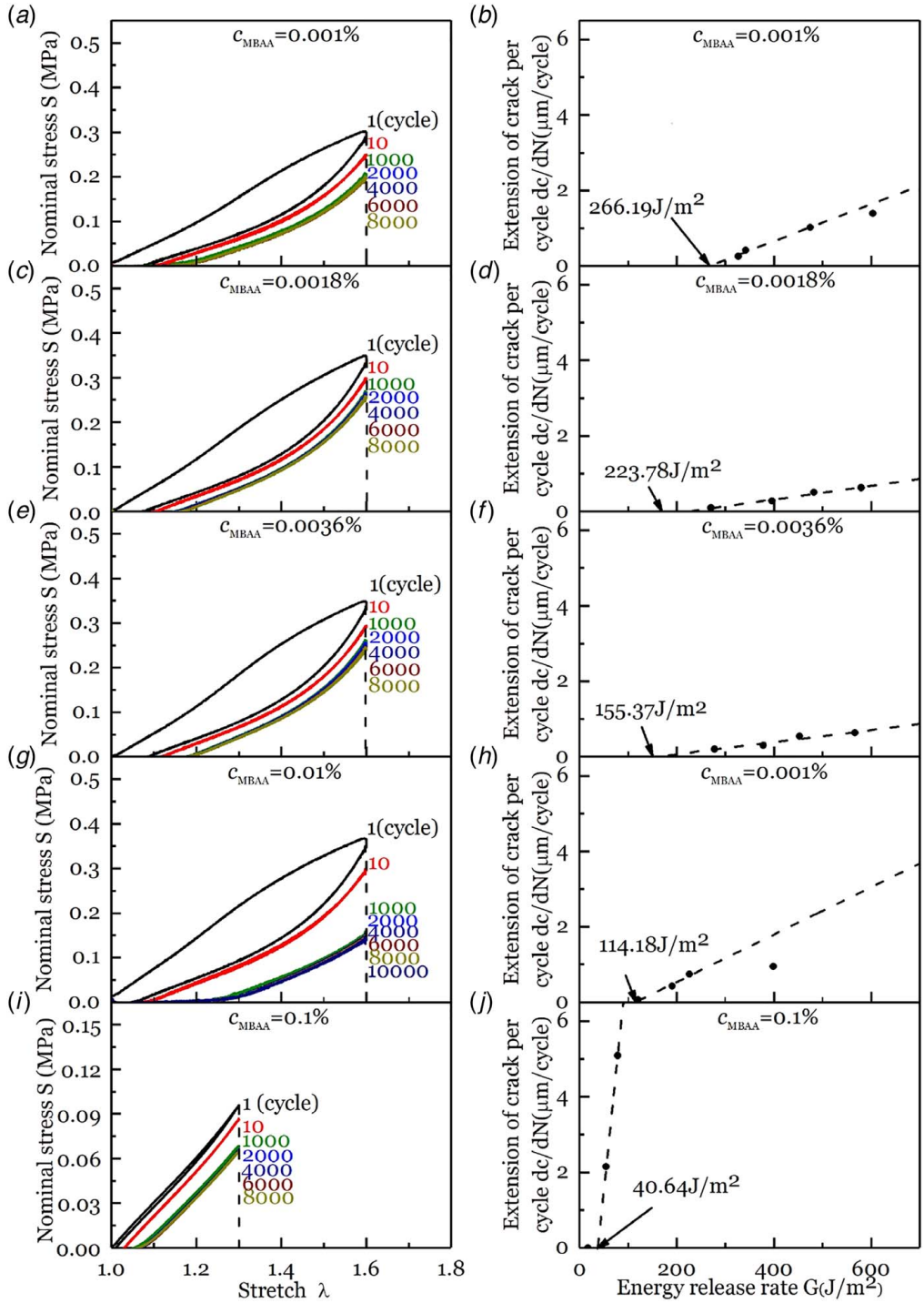

Fig. 5 (a)(c)(e)(g)(i) Stress–stretch curves of the five kinds of hydrogel samples with different PAAm chain lengths under prolonged cyclic loads. (b)(d)(f)(h)(j) The data points on the *G-dc/dN* plane of the five kinds of hydrogel samples are linearly extrapolated to obtain the fatigue threshold. The hydrogel with a longer PAAm chain has a higher fatigue threshold.

m^2 for $c_{MBAA} = 0.0036\%$, 114.2 J/m^2 for $c_{MBAA} = 0.01\%$, and 40.6 J/m^2 for $c_{MBAA} = 0.1\%$. We plot the fatigue threshold as a function of the chain length of the PAAm network in Fig. 12. This result agrees with the theoretical prediction Eq. (1) by the Lake-Thomas model remarkably well. The best fitting gives the constant $C = 1.28$.

We further examine the equation $C = \phi_0^{1/3}\phi^{2/3}\alpha l J/V$. The volume fraction of the PAAm network ϕ_{PAAm} for the five kinds of hydrogel samples was measured using the drying method described above. The volume fraction in the as-prepared state ϕ^0_{PAAm} was not measured in our experiment. We roughly estimate this value as follows. For all the five kinds of samples, the thickness in the fully swollen state is about 1.5 times the thickness in the as-prepared state. The volume change is about $1.5^3 = 3.375$, so that $\phi^0_{PAAm} = 3.375\phi_{PAAm}$. The density of acrylamide ρ is 1.322 g/cm^3. The molecular weight of acrylamide M is 71.08 g/mol. The number of bonds per unit volume of the dry polymer can be estimated by the number of monomers per unit volume of the dry polymer as $b = A\rho/M = 1.12 \times 10^{28}$ m^{-3}, where A is the

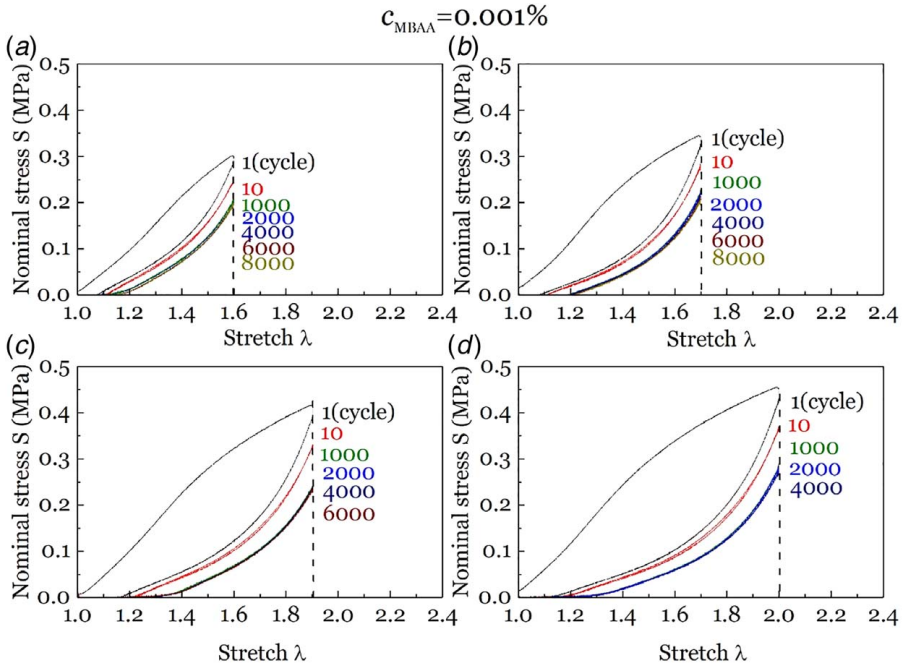

Fig. 6 Stress–stretch curves of the hydrogel samples under prolonged cyclic loads with $c_{MBAA} = 0.001\%$

Avogadro number. The length of a monomer is $l = b^{-1/3} = 0.446$ nm. The energy of a C–C bond U is 3.3×10^{-19} J. The bond energy per unit volume is $J/V = bU = 3.696 \times 10^{9}$ J/m^3. Inserting these numbers into the equation with $C = 1.28$, we obtain the pre-factor α to range from 5.3 to 4.4 for the five kinds of samples with ϕ_{PAAm} ranging from 9.7% to 11.8%.

Figure 2 shows that the stiffness of PAAm-PAMPS double-network hydrogels depends on the chain length of the PAMPS network, $E \sim 1/n_{PAMPS}$. Figure 12 shows that the threshold depends on the chain length of the PAAm network, $\Gamma_0 \sim n_{PAAm}^{1/2}$. These two important indexes for engineering applications, E and Γ_0, are controlled by two independent material parameters, n_{PAMPS} and n_{PAAm}. We plot the data of stiffness and threshold for the five kinds of hydrogels in this paper as well as the data in our previous paper [5,6,23] in the stiffness-threshold diagram (Fig. 13). Compared to the single-network hydrogels at the bottom left region, both stiffness and threshold are significantly improved for double-network hydrogels.

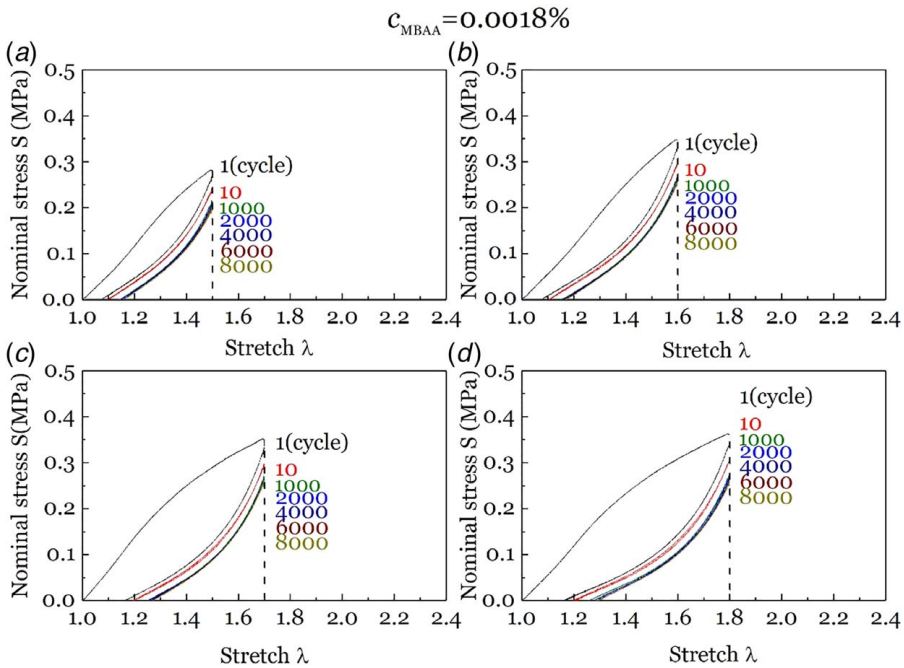

Fig. 7 Stres–stretch curves of the hydrogel samples under prolonged cyclic loads with $c_{MBAA} = 0.0018\%$

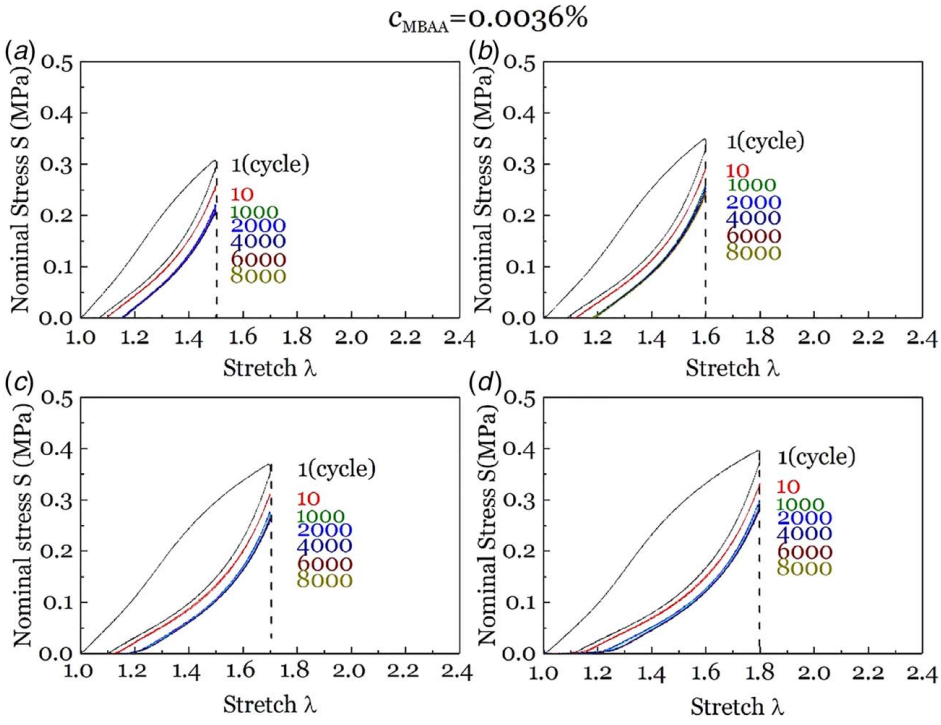

Fig. 8 Stress–stretch curves of the hydrogel samples under prolonged cyclic loads with $c_{MBAA} = 0.0036\%$

If the chain length of the PAMPS network is made shorter, the stiffness of the double-network hydrogel will increase further. However, shorter PAMPS chains will lead to smaller ultimate fracture strains [4]. If the chain length of the PAAm network is made longer, the threshold will increase further in principle. In the specific synthesizing procedure used in this paper, there were always some unreacted crosslinkers when we synthesized the first PAMPS network. Therefore, even we do not add any crosslinker in the second step for the second PAAm network, the double-network hydrogel can still be synthesized [27]. In fact,

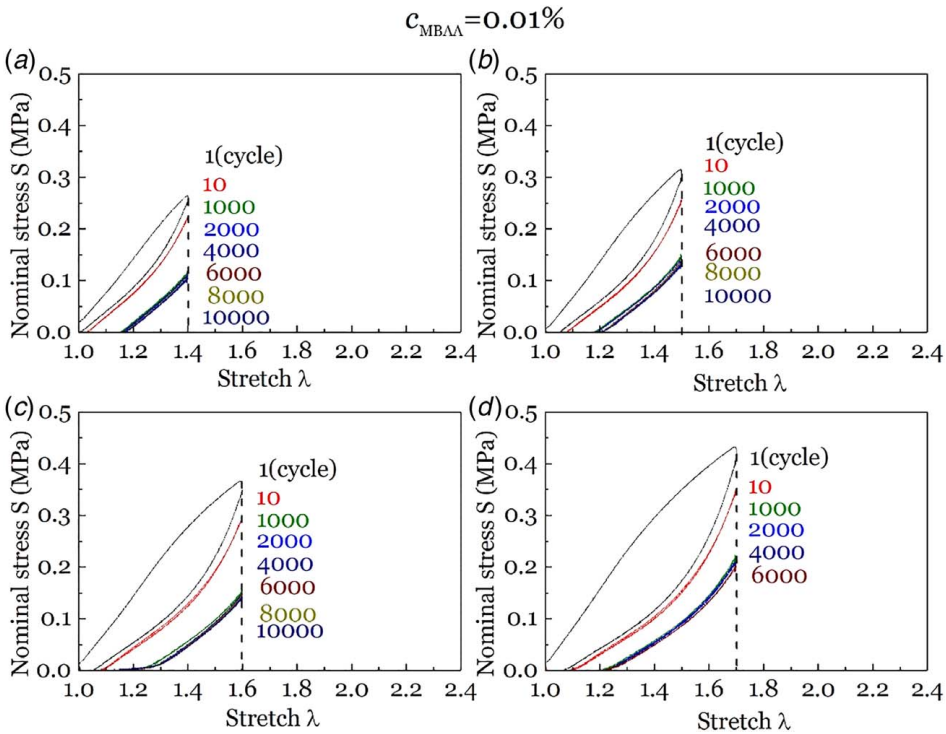

Fig. 9 Stress–stretch curves of the hydrogel samples under prolonged cyclic loads with $c_{MBAA} = 0.01\%$

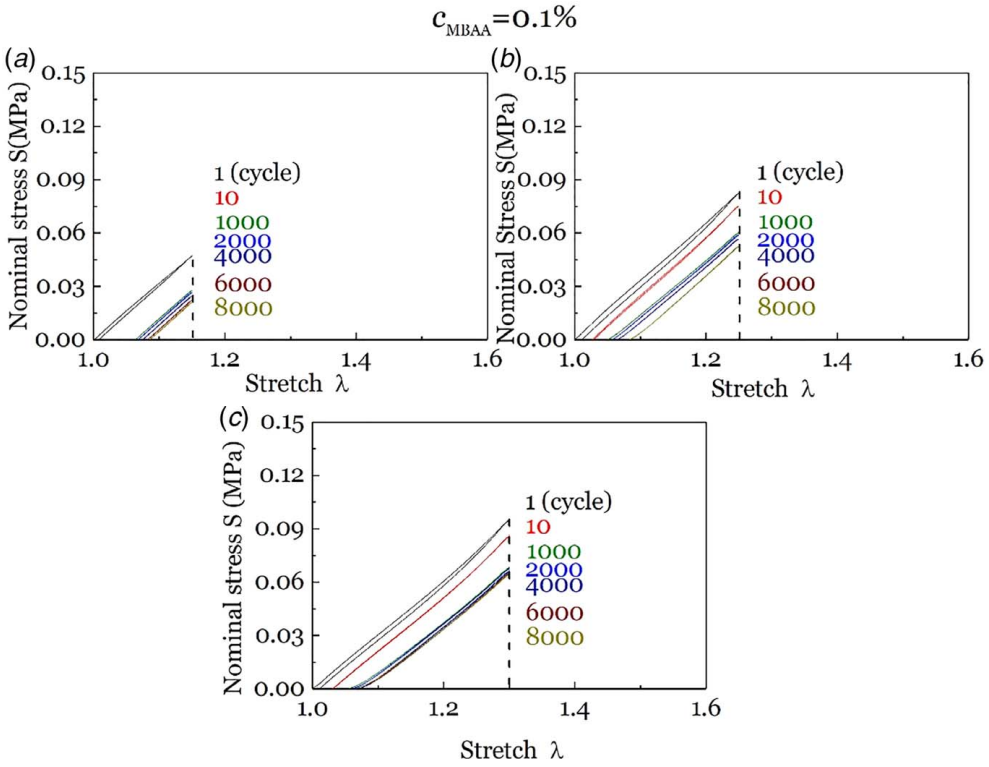

Fig. 10 Stress–stretch curves of the hydrogel samples under prolonged cyclic loads with c_{MBAA} = 0.1%

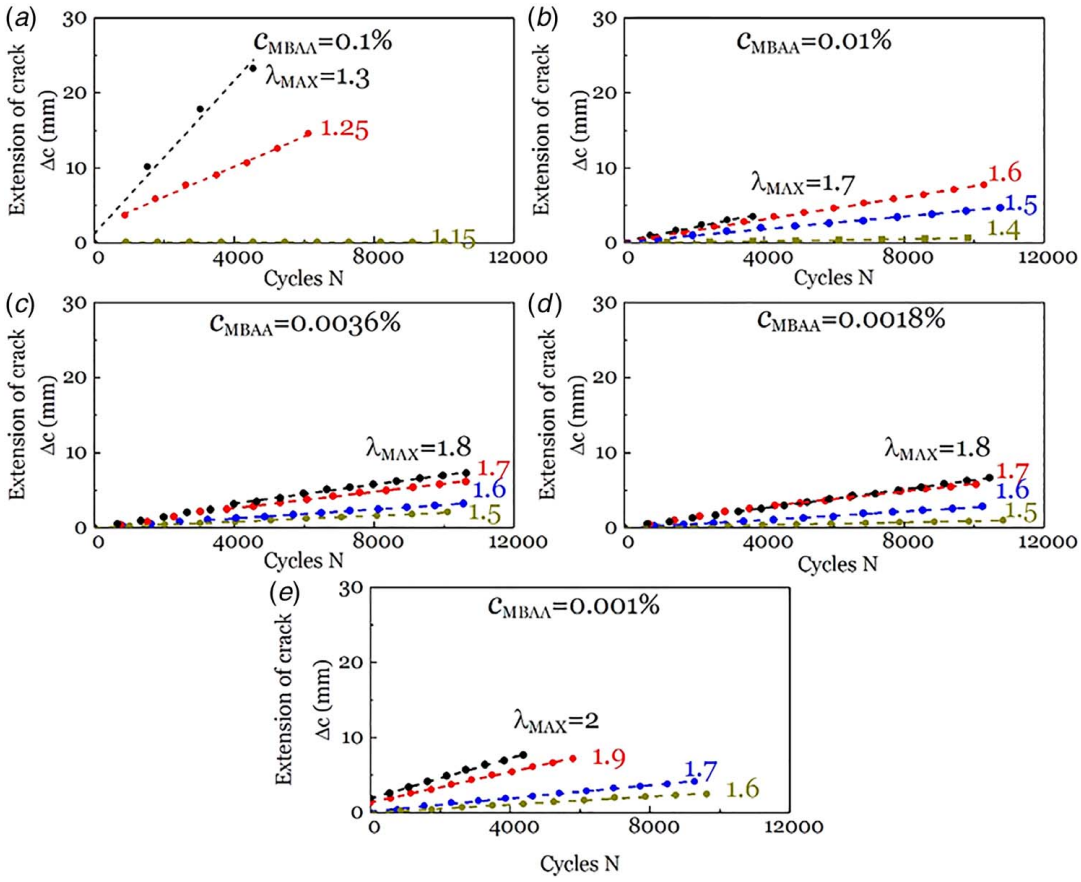

Fig. 11 Extension of crack of the cut samples as a function of the number of cycles under cyclic loads

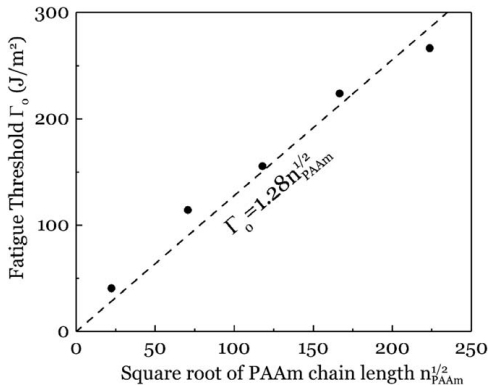

Fig. 12 The chain length dependence of the fatigue threshold of the PAAm-PAMPS double-network hydrogel. The fatigue threshold is proportional to the 1/2 power of the PAAm chain length, as predicted by the Lake-Thomas model.

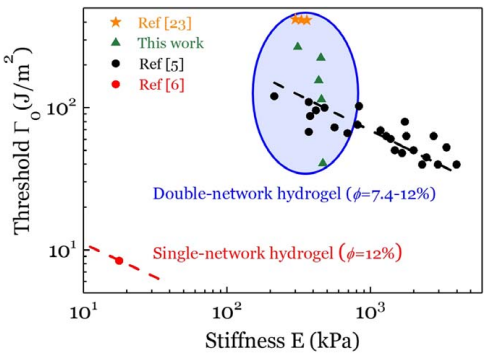

Fig. 13 The stiffness-threshold conflict is resolved in double-network hydrogels. The experimental data of double-network hydrogels show both high stiffness and high threshold.

we have tried this way and repeated all the fracture and fatigue measurements. We find that the threshold can reach 298 J/m^2 when c_{MBAA} in the second step is "zero." This threshold is higher than all other hydrogels tested in this work.

6 Concluding Remarks

Stiffness-threshold conflict exists for single-network elastomers and single-network hydrogels. We show that this conflict can be resolved for double-network materials. We prepared PAAm-PAMPS hydrogels with five different kinds of chain length of the PAAm network. We measured the fatigue damage of the uncut samples and the fatigue fracture of the cut samples under cyclic loads. We demonstrate that the stiffness of PAAm-PAMPS double-network hydrogels depends on the chain length of the PAMPS network as $E \sim 1/n_{PAMPS}$ and the threshold depends on the chain length of the PAAm network as $\Gamma_0 \sim n_{PAAm}^{1/2}$, as predicted by the Lake-Thomas model. The conflict is resolved by separately controlling the chain lengths of the two networks. In designing specific structures in applications, different combinations of material properties such as stiffness, strength, fracture strain, fracture toughness, and fatigue threshold are desired. Tremendous attentions have been paid on the fracture toughness on double-network hydrogels. We now explore another interesting feature of double-network hydrogels, which can serve as a general principle to design hydrogels and elastomers with both high stiffness and high threshold.

Acknowledgment

ZS acknowledges the support of the NSF MRSEC at Harvard (Grant No. DMR-1420570; Funder ID: 10.13039/100000001), and the visiting appointment at Xian Jiaotong University. TL acknowledges the support of NSFC (Grant No. 11772249; Funder ID: 10.13039/501100001809). JH acknowledges the support of NSFC (Grant No. 11702207; Funder ID: 10.13039/501100001809). JT acknowledges the support of NSFC (Grant No. 11702208; Funder ID10.13039/501100001809:) and the Program for Postdoctoral Innovative Talents (No. BX201700192).

References

[1] Treloar, R., 1974, *The Physics of Rubber Elasicity*, Oxford University Press, Oxford.
[2] Lake, G. J., and Thomas, A. G., 1967, "The Strength of Highly Elastic Materials," Proc. R. Soc. London, Ser. A, **300**(1460), pp. 108–119.
[3] Gong, J. P., Katsuyama, Y., Kurokawa, T., and Osada, Y., 2003, "Double-Network Hydrogels With Extremely High Mechanical Strength," Adv. Mater., **15**(14), pp. 1155–1158.
[4] Ahmed, S., Nakajima, T., Kurokawa, T., Anamul Haque, M., and Gong, J. P., 2014, "Brittle–Ductile Transition of Double Network Hydrogels: Mechanical Balance of Two Networks as the Key Factor," Polymer, **55**(3), pp. 914–923.
[5] Bhowmick, A. K., 1988, "Threshold Fracture of Elastomers," J. Macromol. Sci., Part C: Polym. Rev., **28**(3–4), p. 339–370.
[6] Zhang, E., Bai, R., Morelle, X. P., and Suo, Z., 2018, "Fatigue Fracture of Nearly Elastic Hydrogels," Soft Matter, **14**(18), pp. 3563–3571.
[7] Tang, J., Li, J., Vlassak, J. J., and Suo, Z., 2017, "Fatigue Fracture of Hydrogels," Extreme Mech. Lett., **10**, pp. 24–31.
[8] Creton, C., and Ciccotti, M., 2016, "Fracture and Adhesion of Soft Materials: A Review," Rep. Prog. Phys., **79**(4), p. 046601.
[9] Bai, R. B., Yang, J. W., and Suo, Z. G., 2019, "Fatigue of Hydrogels," Eur. J. Mech. A. Solids, **74**, pp. 337–370.
[10] Sun, J. Y., Zhao, X., Illeperuma, W. R., Chaudhuri, O., Oh, K. H., Mooney, D. J., Vlassak, J. J., and Suo, Z., 2012, "Highly Stretchable and Tough Hydrogels," Nature, **489**(7414), pp. 133–136.
[11] Takashima, Y., Otani, K., Kobayashi, Y., Aramoto, H., Nakahata, M., Yamaguchi, H., and Harada, A., 2018, "Mechanical Properties of Supramolecular Polymeric Materials Formed by Cyclodextrins as Host Molecules and Cationic Alkyl Guest Molecules on the Polymer Side Chain," Macromolecules, **51**(16), pp. 6318–6326.
[12] Chen, Y., and Shull, K. R., 2017, "High-Toughness Polycation Cross-Linked Triblock Copolymer Hydrogels," Macromolecules, **50**(9), pp. 3637–3646.
[13] Li, J., and Mooney, D. J., 2016, "Designing Hydrogels for Controlled Drug Delivery," Nat. Rev. Mater., **1**(12), p. 16071.
[14] Zhang, Y. S., and Khademhosseini, A., 2017, "Advances in Engineering Hydrogels," Science, **356**(6337), p. eaaf3627.
[15] Beebe, D. J., Moore, J. S., Bauer, J. M., Yu, Q., Liu, R. H., Devadoss, C., and Jo, B. H., 2000, "Functional Hydrogel Structures for Autonomous Flow Control Inside Microfluidic Channels," Nature, **404**(6778), pp. 588–590.
[16] Sidorenko, A., Krupenkin, T., Taylor, A., Fratzl, P., and Aizenberg, J., 2007, "Reversible Switching of Hydrogel-Actuated Nanostructures Into Complex Micropatterns," Science, **315**(5811), pp. 487–490.
[17] Keplinger, C., Sun, J. Y., Foo, C. C., Rothemund, P., Whitesides, G. M., and Suo, Z., 2013, "Stretchable, Transparent, Ionic Conductors," Science, **341**(6149), pp. 984–987.
[18] Sun, J. Y., Keplinger, C., Whitesides, G. M., and Suo, Z., 2014, "Ionic Skin," Adv. Mater., **26**(45), pp. 7608–7614.
[19] Wirthl, D., Pichler, R., Drack, M., Kettlguber, G., Moser, R., Gerstmayr, R., Hartmann, F., Bradt, E., Kaltseis, R., Siket, C. M., Schausberger, S. E., Hild, S., Bauer, S., and Kaltenbrunner, M., 2017, "Instant Tough Bonding of Hydrogels for Soft Machines and Electronics," Sci. Adv., **3**(6), p. e1700053.
[20] Yang, C. H., and Suo, Z. G., 2018, "Hydrogel Ionotronics," Nat. Rev. Mater., **3**(6), pp. 125–142.
[21] Gong, J. P., 2010, "Why Are Double Network Hydrogels So Tough?" Soft Matter, **6**(12), pp. 2583–2590.
[22] Zhang, W. L., Liu, X., Wang, J. K., Tang, J. D., Hu, J., Lu, T. Q., and Suo, Z. G., 2018, "Fatigue of Double-Network Hydrogels," Eng. Fract. Mech., **187**, pp. 74–93.
[23] Bai, R. B., Yang, J. W., Morelle, X. P., Yang, C. H., and Suo, Z. G., 2018, "Fatigue Fracture of Self-Recovery Hydrogels," ACS Macro Lett., **7**(3), pp. 312–317.
[24] Zhang, W. L., Hu, J., Tang, J. D., Wang, Z. T., Wang, J. K., Lu, T. Q., and Suo, Z. G., 2018, "Fracture Toughness and Fatigue Threshold of Tough Hydrogels," ACS Macro Lett., **8**(1), pp. 17–23.
[25] Rivlin, R. S., and Thomas, A. G., 1953, "Rupture of Rubber. I. Characteristic Energy for Tearing," J. Polym. Sci., **10**(3), pp. 291–318.
[26] Thomas, A. G., 1958, "Rupture of Rubber. V. Cut Growth in Natural Rubber Vulcanizates," J. Polym. Sci., **31**(123), pp. 467–480.
[27] Nakajima, T. F. H., Tanaka, Y., Kurokawa, T., Osada, Y., and Gong, J. P., 2009, "True Chemical Structure of Double Network Hydrogels," Macromolecules, **42**(6), pp. 2184–2189.